Technical Paper

ISSN 1997-1400 Int. J. Pavement Res. Technol. 8(3):167-171

Intrinsic Roughness Mitigation of Pavements on Expansive Soils – an Analytic Investigation

Eyal Levenberg[1+]

Abstract: Pavements resting on active clays are exposed to uneven heaving and shrinking of their bottom boundary. This paper investigated the inherent ability of pavements to mitigate such underlying (core) roughness. The problem is addressed and analyzed with an analytic model. It is found that the combined thicknesses of all inert pavement layers govern this smoothing feature. Core wavelengths that are much larger compared to the aforementioned thickness are essentially mirrored at the surface. Conversely, core wavelengths shorter than the system's thickness are attenuated. The information included in this work can serve as an additional (and rational) decision basis for the design and evaluation of pavements on expansive soils.

DOI: 10.6135/ijprt.org.tw/2015.8(3).167
***Key words**: Active clay; Elastic theory; Pavement design; Roughness; Subsurface deformation.*

Introduction

In the presence of a pavement, direct water infiltration into the underlying soil is essentially prevented; moisture evaporation is also considerably diminished. Because of this, changes in subterranean water contents commence subsequent to any new construction [1, 2]. These changes take place within the so-called 'active zone'; they are rather slow-occurring, governed by capillarity and short-range adsorption forces [3, 4]. Without providing conditions for long-term equilibrium under the pavement, i.e., purposefully preventing moisture from entering or escaping from the top and edges, water contents will continue to fluctuate in response to climate all through the system's service life.

In case of active clays, such moisture oscillations lead to swelling and shrinking deformations. Due to spatial variability in both soil properties and initial moisture conditions, the resulting deformations are uneven. Consequently, pavements resting on expansive soils are subjected to a distorting bottom boundary. The powerful propensity for volume change exhibited by active clays, and the fact that pavements are relatively lightweight, imply that the movements are essentially 'prescribed'. Nonetheless, common engineering design policies call for 'thickening' the system in an effort to cope with the problem [5]. The approach aims at counteracting swelling with added weight from inert layers; it is conceptually supported by so-called one-dimensional Potential Vertical Rise (PVR) procedures. These were pioneered during the 1950's by McDowell [6] and further developed in subsequent years [7-9]; an updated literature survey on the topic is included in [10]. Naturally, subsidence due to shrinking cannot be counteracted according to the PVR scheme.

There exists some engineering evidence that the 'thickening' policy may be advantageous for coping with core (subsurface) roughness. The advantage is neither related to neutralizing clay movements, nor is it related to improved climatic isolation of the underlying soil. It is related to the system's inherent ability to modify and alleviate subsurface mounds and depressions so that the waviness will not be duplicated at the surface. A noteworthy work in this connection is by McKeen [11], who developed a design method for airport pavements in expansive soils.

As part of the McKeen's work, profile wavelengths and amplitudes were compared between uncovered soils and nearby paved surfaces. While wavelengths were essentially similar (i.e., within similar ranges), the amplitudes were generally smaller in the paved cases. An analytical treatment was also suggested for capturing the aforementioned effect wherein the pavement was modeled as a long beam resting on a bed of springs (i.e., Winkler foundation). Roughness was introduced by distorting the bottom end of the springs, which in turn generated deformation in the beam. In the analyses, a downward distortion was imposed for simulating a non-uniform shrinking subgrade profile. Then after, differences between maximum settlement at the beam surface and maximum imposed spring displacement were calculated for a range of wavelengths.

A final chart was provided by McKeen, relating the beam's 'smoothing' ability to the applied depression wavelength normalized by the characteristic length of the problem. The latter involves the beam's flexural stiffness which is proportional to the thickness cubed as well as the assumed modulus of subgrade reaction. While simplistic, and somewhat unrealistic, the 'beam' model created a direct link between roughness moderation capacity and equivalent pavement thickness. The latter was computed by conversion of actual layer thicknesses into an overall thickness for a single material that exhibits an equivalent flexural rigidity.

Another noteworthy work in this connection is by Velsco and Lytton [12] who measured and analyzed ride surface roughness in pavements resting on expansive soils. The recorded profiles were decomposed into a spectrum of sine wave amplitudes and associated wavelengths. Subsequently, by means of regression, the spectrum in each surveyed section was fitted to a power law expression. Across all investigated cases, the involved constants were found to depend, among other factors, on the effective thickness of the pavement.

[1] Technion - Israel Institute of Technology, Technion City, Haifa 32000, Israel.
[+] Corresponding Author: E-mail elevenbe@technion.ac.il
Note: Submitted October 7, 2014; Revised February 29, 2015; Accepted March 7, 2015.

The current work may be considered as an improved and as a modern analytic version of the abovementioned modeling efforts. It is based on linear (layered) elasticity theory, a widely practiced and familiar framework for pavement engineers. The purpose here is to expose and analyze the intrinsic capacity of a pavement system to mitigate roughness imposed from the bottom boundary. An existing three-dimensional model, recently developed by the author, is employed [13]. Herein, part of the original formulation is first reiterated, slightly expanded, and then interrogated numerically to produce curves of engineering worth. A fictitious case is subsequently presented for demonstrating the findings and also for demonstrating the simple and straightforward usage of the curves - in anticipation that they gain practical acceptance.

Modeling and Analysis

This section is concerned with calculating the surface displacements of a pavement due to an imposed subsurface deformation. The pavement system is modeled as a two-layered linear elastic weightless half-space; each layer is homogeneous and isotropic. The top layer, with finite thickness *H*, represents the pavement structure as well as any inert subgrade layers; it is characterized by a single set of elastic properties: Young's modulus *E* and Poisson's ratio *v*. For a multilayered system, this thickness can be understood as an equivalent thickness (similarly to the classic treatment). The bottom layer, with semi-infinite thickness, represents the expansive soil. A cylindrical coordinate system is used with its origin placed at the top boundary, the *r*-axis ($r \geq 0$) parallel to it, and the *z*-axis drawn into the medium

The surface of this model pavement is completely stress-free and unrestricted to deform. Also, at the interface between the layers, zero shear stresses are prescribed to simulate the presence of a horizontal moisture barrier membrane [14]. The model is 'loaded' by vertically displacing the bottom of the finite layer (i.e., where *z* = *H*), simulating the effect of an expansive soil. Such a Dirichlet type boundary condition renders the elastic properties of the semi-infinite (bottom) layer irrelevant. An axisymmetric bulge or a localized heave-type deformation is specified, mathematically written as a two-dimensional Gaussian:

$$u_z^H(r) = q_H e^{-(r/a_H)^2/2} \tag{1}$$

in which $u_z^H(r)$ is the magnitude of the prescribed movement at a radial distance *r* from the symmetry axis, q_H is the peak displacement (negative = upward) occurring at the center where *r* = 0, and a_H is referred to herein as the 'width' of the Gaussian; it denotes the point of inflection w.r.t. the radial coordinate, i.e., $d^2u_z^H/dr^2 = 0$ when *r* = a_H. The particular choice of Eq. (1) was inspired by studies dealing with ground subsidence resulting from tunneling [15]. Nonetheless, it can serve as a radial basis function for expressing any two-dimensional shape of interest [16].

Solving the elasticity equations with the imposed boundary conditions gives, as shown in [13], an analytically exact expression for the vertical surface deformation $u_z^0(r)$:

$$u_z^0(r) = -H(1+\nu)\int_{m=0}^{\infty} J_0\left(\frac{mr}{H}\right)\left(Ae^{-m} - B - C(2-4\nu)e^{-m} - D(2-4\nu)\right)dm \tag{2}$$

where *m* is a unitless integration parameter, J_0 is the Bessel function of the first kind of order zero, and *A*, *B*, *C*, and *D* are each a function of *m* obtained from the following expressions:

$$A = (2\nu + m - 2\nu e^{-2m} - me^{-2m} + 4m\nu e^{-2m})F \tag{3}$$

$$B = e^{-m}(m - 2\nu + 2\nu e^{-2m} - me^{-2m} - 4m\nu)F \tag{4}$$

$$C = (e^{-2m} - 1 - 2me^{-2m})F \tag{5}$$

$$D = e^{-m}(e^{-2m} - 1 - 2m)F \tag{6}$$

in which:

$$F = \frac{-q_H a_H^2 m e^{-(ma_H)^2/2H^2}}{2H^3(1-\nu^2)(1+4me^{-2m}-e^{-4m})} \tag{7}$$

Careful study of Eq. (2) revealed that the resulting deformation at the free surface can also be approximated as a two-dimensional axisymmetric Gaussian [13]:

$$u_z^0(r) \approx q_0 e^{-(r/a_0)^2/2} \tag{8}$$

where q_0 denotes the peak vertical deformation, occurring at the symmetry axis (where *r* = 0), and a_0 is the width of the resulting surface 'bulge'.

A sketch of the model with all abovementioned elements is shown in Fig. 1. The original (undeformed) surface and subsurface boundaries are indicated with dash-dot lines that are parallel to each other and separated by the thickness *H*. The imposed subsurface deformation is indicated with a solid line and vertical arrows; the associated Gaussian shape parameters q_H and a_H are clearly indicated. The resulting (surface) deformation is denoted by a dashed line, characterized by Gaussian parameters q_0 and a_0. Intentionally, q_0 was drawn smaller than q_H and a_0 was drawn larger than a_H. This is the essence of the roughness mitigation capability; the core distorting shape is 'softened' at the surface.

Fig. 2 presents the relationship established between the 'applied' q_H and the resulting q_0, and also between the subsurface Gaussian width a_H and the resulting (surface) Gaussian width a_0. In the figure, the ratios q_0/q_H and a_0/a_H are plotted against the ratio H/a_H. It is important to note that the curves are unique, blind to the deformation direction (i.e., applicable to either swell or shrink deformation), independent of the actual (physical) dimensions utilized in the calculations, and most importantly independent of the top layer's elastic properties. This latter outcome somewhat justifies the single-layer modeling simplification.

In the figure, as H/a_H varies between 0 and 10, the ratio q_0/q_H monotonically decreases from an initial value of unity to 0.049. At the same time, the ratio a_0/a_H monotonically increases from unity to a value of 4.424. This behavior quantifies the roughness mitigation capability of the pavement; given q_H and a_H values, Fig. 2 offers a quantitative estimate for q_0 and a_0 depending on the

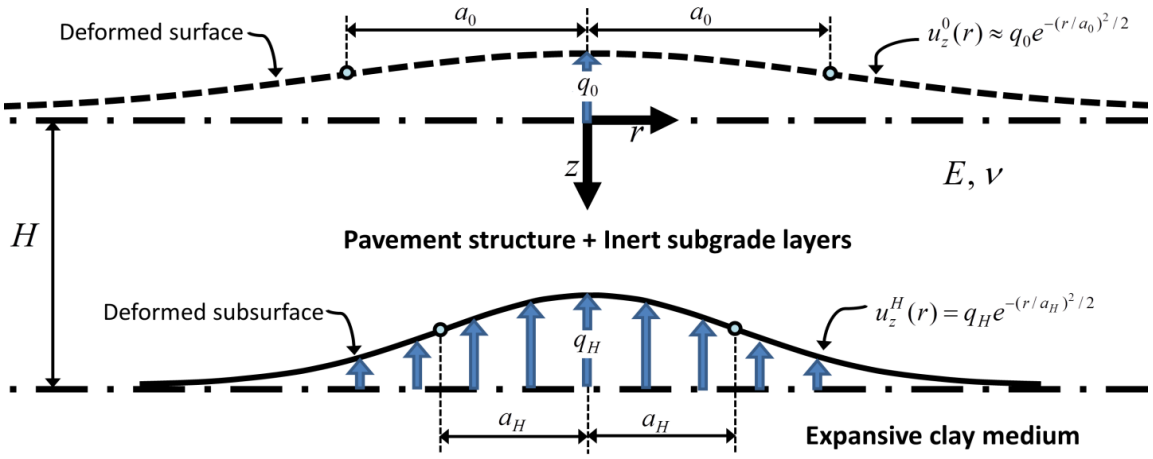

Fig. 1. Cross-sectional View of Model Elements.

choice of H. A pavement that is relatively thin, with H < a_H (or equivalently H / a_H < 1), will practically mirror the distorted subsurface shape onto the surface, i.e., $q_0 \approx q_H$ and $a_0 \approx a_H$. Roughness mitigation essentially commences for thicker pavements, characterized by H > a_H; in this case, the substrate bulge is 'stretched' and its peak attenuated.

Demonstrative Application

The previous section provided a very simple and direct link between a localized subsurface heaving (or sagging) and a resulting surface displacement. This information can be utilized by engineers to analyze any core deformation shape of interest. In order to achieve this, a sum of Gaussians must first be used to express substrate movements:

$$u_z^H(x,y) = \sum_{j=1}^{N} q_{H,j} e^{\frac{(x-X_j)^2+(y-Y_j)^2}{-2(a_{H,j})^2}} \quad (9)$$

where $u_z^H(x,y)$ is any geometry of imposed vertical displacement, expressed using a Cartesian system with coordinates x and y. This core geometry comprises a sum of N axisymmetric Gaussians, each identified by a subscript j. Shape parameters of the jth Gaussian include: peak displacement $q_{H,j}$, width $a_{H,j}$, and spatial coordinates of the symmetry axis X_j and Y_j. Once this array of Gaussians is determined, and based on a chosen pavement thickness, the surface deformation caused by the jth Gaussian can be easily accessed from Fig. 2. All that is required for this purpose is swapping Gaussian attributes in Eq. (9) and recalculating, i.e., $q_{0,j}$ instead of $q_{H,j}$ and $a_{0,j}$ in place of $a_{H,j}$.

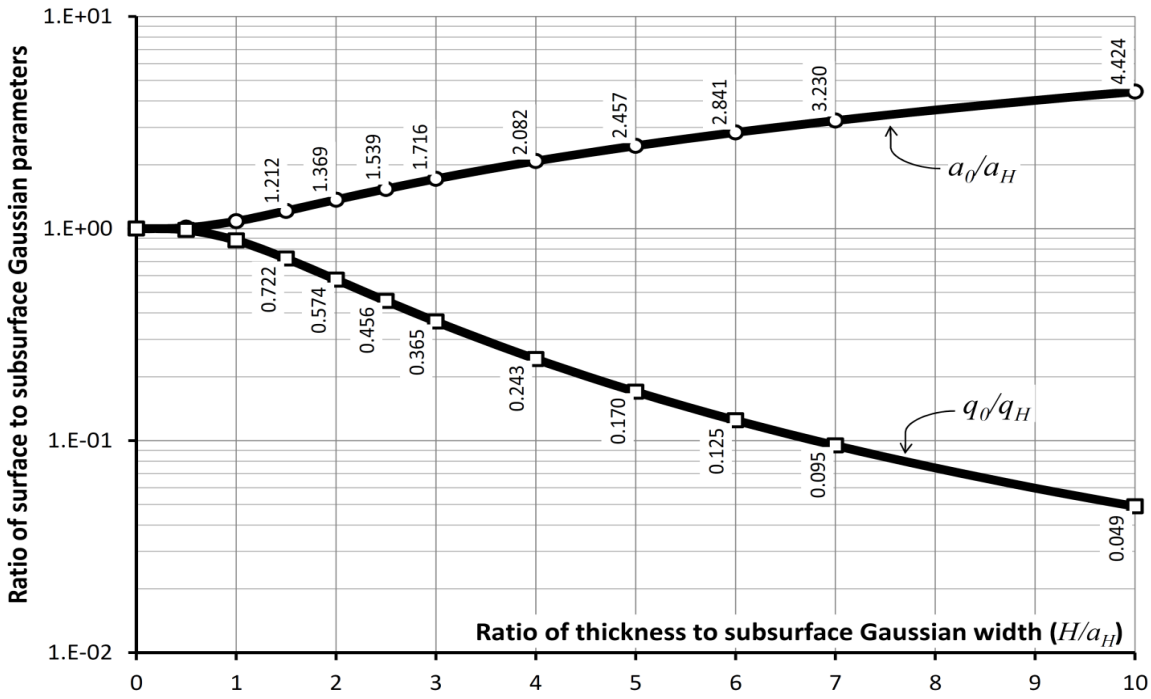

Fig. 2. Theoretical Relation between Surface Deformation and Imposed Subsurface Bulge as a Function of Pavement Thickness.

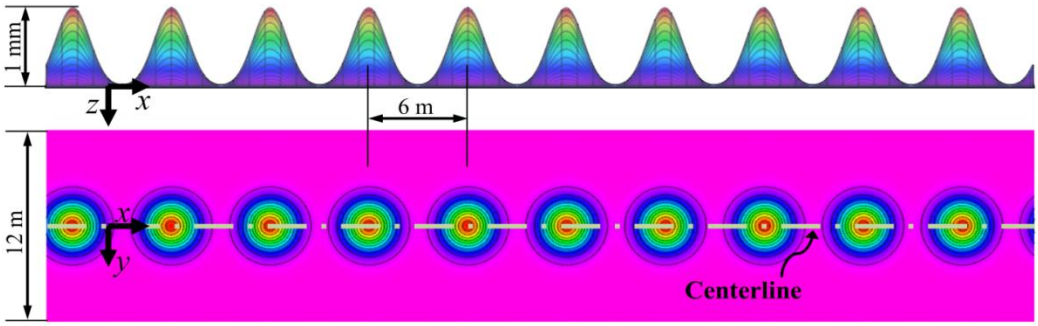

Fig. 3. Imposed Subsurface Bulge Pattern as a Sum of Spatially Distributed Gaussians; Side View (Upper Chart) and Top View (Lower Chart).

As means of demonstrating this procedure, a long fictitious pavement strip, 12 m wide, was considered. Fig. 3 shows the deformed subsurface, offering both side and top views. The imposed geometry was represented by a series of identical Gaussians spaced 6,000 mm apart in the longitudinal direction with their symmetry axes located along the strip centerline. Each Gaussian was characterized by q_H = 1 mm and a_H = 1000 mm. These attributes resulted in near pure haversine deformation pattern longitudinally, and heave-type unevenness transversely. For this particular parameter choice, the resulting profile along the centerline had a wavelength of 6 m and amplitude of 0.5 mm. Other combinations of wavelength and amplitude may be reproduced by such series of Gaussians. For this purpose the spacing between the symmetry axes should remain equal to the requested wavelength, the q_H shape parameter should equal twice the desired amplitude, and the width parameter a_H should equal about one sixth of the wavelength.

Fig. 4 presents the imposed deformation for an arbitrary section along the strip centerline (solid line); the sinusoidal pattern can clearly be seen. Also included in Fig. 4 are three different surface displacements, each associated with a different pavement thickness. As can be expected, the ride surface roughness is sinusoidal in shape with a wavelength that is identical to that imposed upon the subsurface. However, as can be seen, the deformation amplitude is attenuated depending on the chosen pavement thickness. For $H = 1.5a_H = 1.5$ m (dotted line), the surface amplitude reduces to 65% of that which is imposed; for $H = 2.0a_H = 2.0$ m (dashed line) the surface amplitude reduces to 47% of that imposed, and when $H = 2.5a_H = 2.5$ m (dash-dot line) the surface amplitude reduces to 37% of the core amplitude. Therefore, the intrinsic ability of pavements to mitigate roughness in expansive soils is demonstrated.

Summary and Comments

Pavements on expansive soils are exposed to an unevenly distorting bottom boundary. Consequently, the mounds and the depressions are reflected onto the riding surface generating longitudinal roughness and transverse waviness. An existing analytical formulation developed in [13] was reiterated, slightly expanded, and subsequently employed to investigate this problem. A single elastic layer was employed here to represent the pavement structure along with any inactive subgrade layers. Quantified first was the surface deformation response due to a subsurface axisymmetric bulge (or sag); this response was studied as a function of pavement thickness. From this basic solution, arbitrary distortion shapes can be reproduced and analyzed by spatially superposing several axisymmetric cases.

The computational scheme is mathematically exact, and therefore applies to field conditions provided the underlying assumptions are satisfied. In this connection it is reasonable to assume that all pavement layers exhibit near-linear response - especially when deformations are slow occurring and no transient (and localized) traffic loads are considered [13, 17]. It was shown that thickness governs the ability of a pavement to mitigate roughness. In the case of thin pavements, subsurface humps (or sags) are essentially duplicated onto the surface. On the other hand, thicker pavements 'stretch' the width of a subsurface bulge (or depression) and attenuate its peak deformation, effectively smoothing any imposed roughness.

Qualitatively, these results are completely in tune with the field measurements reported by McKeen [11] and Velsco and Lytton [12] (refer to the Introduction section). They also coincide with the work of McKeen [18], who presented and analyzed roughness measurements taken from six different airport sites. According to the terminology in the current work, surveyed (equivalent) pavement thicknesses (H values) ranged from 0.17 to 0.82 m while Gaussian width parameters (a_H values) ranged from 0.9 to 1.8 m (i.e., one sixth of the reported wavelength). In all 15 pavement systems mentioned, the ratio H / a_H was rather low, between 0.15 and 0.64, which translates into minimal roughness mitigation based on Fig. 2. As expected, the roughness performance for 13 out of the 15 surveyed cases was rated as unsatisfactory [18]. It is noteworthy that the two pavements receiving a "satisfactory" roughness rating were the ones with the highest H / a_H rations.

Overall, the information included in this paper can serve as a rational decision basis when choosing a 'treatment depth' for pavements in active clays. One approach is to commence by estimating a_H and q_H for the site. These entities are essentially linked to subsoil characteristic wavelength and amplitude (respectively); both may be obtained from existing correlations with active zone depth (z_a), suction compression index (C_h), and coefficient of variation in C_h [11, 18]. Then, for any trial choice of H, Fig. 2 and Eq. (9) allow ride-surface roughness quantification.

Other potential uses of the theory and Fig. 2 curves include analysis of adverse effects upon ride quality due to unstable buried utilities, growing tree roots, or freeze-thaw cycles. Another possible

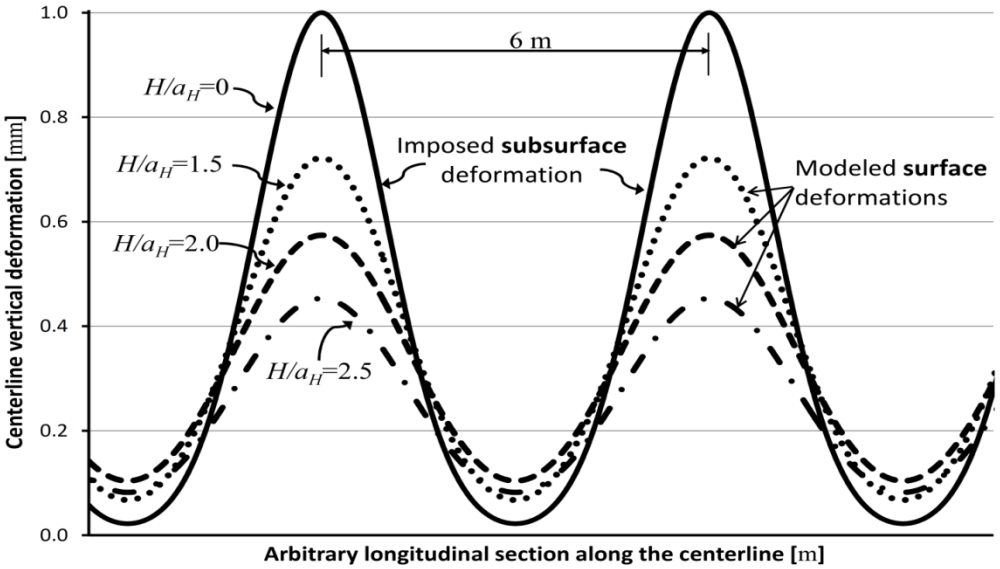

Fig. 4. Roughness Mitigation for Different Pavement Thicknesses in Fictitious Pavement Strip (See Fig. 3).

application is performing an inverse type of analysis to backcalculate subsurface movements in existing pavements based on observable surface measurements. Exploring these ideas should contribute to the development of a mechanistic framework for pavement roughness.

References

1. Fityus, S.G., Smith, D.W., and Allman, M.A. (2004). Expansive Soil Test Site near Newcastle, *Journal of Geotechnical and Geoenvironmental Engineering*, 130(7), pp. 686-695.
2. Aitchison, G.D. (1965). Statement of the Review Panel: Engineering Concepts of Moisture Equilibria and Moisture Changes in Soils Beneath Covered Area, *Proceedings of the Moisture Equilibria and Moisture Changes in Soils Beneath Covered Areas symposium*, Butterworths, Australia, pp. 7-21.
3. Holtz, R.D. and Kovacs, W.D. (1981). *An Introduction to Geotechnical Engineering*, Prentice-Hall, Inc., Englewood Cliffs, NJ, USA.
4. Lu, N. and Likos, W.J. (2004). *Unsaturated Soil Mechanics*, Wiley, New York.
5. Tex-124-E (2014). Test Procedure for Determining Potential Vertical Rise, Construction Division of the Texas Department of Transportation (TxDOT), Austin, Texas, USA.
6. McDowell, C. (1956). Interrelationship of Load, Volume Change, and Layer Thickness of Soils to the Behavior of Engineering Structures, *Proceedings of the 35th Highway Research Board Annual Meeting*, pp. 754-770.
7. Lytton, R.L. and Watt, W.G. (1970). Prediction of Swelling in Expansive Clays, Center for Highway Research, Report Number 118-4, University of Texas at Austin, TX, USA.
8. Briaud, J.L., Zhang, X., and Moon, S. (2003). Shrink Test-Water Content Method for Shrink and Swell Predictions, *Journal of Geotechnical and Geoenvironmental Engineering*, 129(7), pp. 590-600.
9. Fityus, S.G., Cameron, D.A., and Walsh, P.F. (2005). The Shrink Swell Test, *Geotechnical Testing Journal*, 28(1), pp. 1-10.
10. Vanapalli, S.K. and Lu, L. (2012). A State-of-the Art Review of 1-D Heave Prediction Methods for Expansive Soils, *International Journal of Geotechnical Engineering*, 6, pp. 15-41.
11. McKeen, R.G. (1981). Design of Airport Pavements for Expansive Soils, New Mexico Engineering Research Institute, Report *DOT/FAA/RD-81-25*, University of New Mexico, Albuquerque, NM, USA.
12. Velsco, M.O. and Lytton, R.L. (1981). Pavement Roughness on Expansive Clays, Texas Transportation Institute, Report *FHWA/TX-81/3-284/2*, Texas A&M University, College Station, TX, USA.
13. Levenberg, E. (2013). Analysis of Pavement Response to Subsurface Deformations, *Computers and Geotechnics*, 50, pp. 79-88.
14. Nelson, J.D. and Miller, D.J. (1992). *Expansive Soils: Problems and Practice in Foundation and Pavement Engineering*, John Wiley & Sons, Inc, New York, USA.
15. Peck, R.B. (1969). Deep Excavations and Tunnels in Soft Ground, *Proceedings of the 7th International Conference on Soil Mechanics and Foundation Engineering*, Mexico City, State of the Art Volume, pp. 225-290.
16. Goshtasby, A. and O'Neill, W.D. (1993). Surface Fitting to Scattered Data by a Sum of Gaussians, *Computer Aided Geometric Design*, 10, pp. 143-156.
17. Levenberg, E. and Garg, N. (2014). Estimating the Coefficient of At-Rest Earth Pressure in Granular Pavement Layers, *Transportation Geotechnics*, 1(1), pp. 21-30.
18. McKeen, R.G. (1985). Validation of Procedures for Pavement Design on Expansive Soils, Report *DOT/FAA/PM-85/15*, University of New Mexico, Albuquerque, NM, USA.